COMBINING GTD WITH MOM IN ANALYSING THE SCATTERING FROM THE LICEF ANTENNAS ON THE SMOS SATELLITE

Frank Jensen, Knud Pontoppidan

TICRA, Laederstraede 34-2, DK-1201 Copenhagen K, Denmark, Emails: fj@ticra.com and kp@ticra.com

ABSTRACT

The present paper describes the determination of the scattering from the LICEF antenna elements on the SMOS satellite taking into account that the solar panels rotate during the flight of the satellite.

The task is well suited for a ray analysis based on the Uniform Geometrical Theory of Diffraction (GTD) since this method is fast which is essential due to the time varying scattering structure. However, the source antennas are mounted in deployable arms which interact with the antenna elements and shields for the direct illumination of the satellite body and the solar panels.

GTD is not suited for determining the scattering in structures very close to the source antenna. The scattering in these structures may then be solved by the Method of Moments (MoM). On the other hand the full structure is too large to be handled by MoM.

The paper describes how the two methods are combined, especially the problem of delimiting the structures handled by MoM from the structures handled by GTD as the latter must be in the far field of the former while they nevertheless are connected parts of the same satellite structure.

The scattering in the satellite and especially in the solar panels are then determined. First, stationary full sphere patterns for different antenna elements and different orientations of the solar panels have been calculated and next, the sun radiation into the elements is determined as function of time for typical satellite orbits taking into account the scattering in the structure, with the solar panels fixed or oriented to maximum power absorption.

1. INTRODUCTION

In this paper we describe the determination of the scattering from the LICEF antenna elements on the SMOS satellite (measuring Soil Moisture and Ocean Salinity, Fig. 1) taking into account that the solar panels rotate during the flight of the satellite. Originally, the satellite was planned to have fixed solar panels but the power budget is improved if the solar panels are rotated to maximum sun incidence.

The purpose of the antenna is to measure the emission from the earth. It is therefore sensitive to stray radiation from other sources. The background for the study has been to investigate if the antenna was more sensitive for receiving noise from the sun when the solar panels are rotating than when the panels are fixed. The work has been carried out for ESA[1] and is reported in [1].
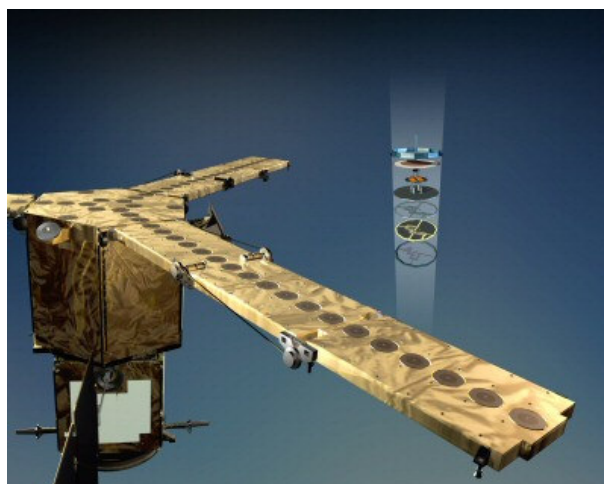

Figure 1. SMOS, artist's impression (ESA). Two of the three arms with the 69 LICEF antenna elements of which one is shown in exploded view.

For determination of the scattering in a large structure such as a satellite a ray analysis by the Uniform Geometrical Theory of Diffraction (GTD) is well suited. Further, the method is fast which is essential when the scattering structure changes dynamically.

A principle of GTD is that the power radiates along rays and the scatterers are assumed in the far field of the source. This is a problem when the radiating antenna is close to parts of the scattering structure as for SMOS where the antenna elements are embedded in the supporting arms.

In such cases the Method of Moments (MoM) is a better choice. This method is based on the solution of a matrix equation method and is very accurate, but the requirements for the computation time and storage increases drastically with the overall size of the modelled scatterer for which reason the method can not be applied for the full satellite structure.

---

[1] The work has been carried out for ESA on ESTEC contract 11514/05/NL/FF.

A combination of the two methods is therefore advantageous. The source antenna and its close surroundings shall be handled by MoM and so shall the scattering in the satellite body. The scattering in the rotating solar panels may then be handled by GTD.

The challenge of this combination is to separate the radiating structure from the scattering structures. The MoM model will determine currents on the modelled structure, and only on this. This means that the long arm in which the antenna elements are embedded must be suitably truncated in a short section which is interacting with the actual source antenna element and a remaining length with negligible currents. The currents on the short section will be part of the source in the GTD calculations. The size of the GTD source thus increases according to the structure included in the MoM modelling and it becomes more difficult to fulfil the assumption in GTD, that the scattering structures are in the far field of the source.

2.   GEOMETRY

The LICEF antenna elements operates in the frequency band from 1400 MHz to 1427 MHz with a centre frequency at 1413.5 MHz corresponding to the wavelength $\lambda = 212$ mm.

The modelling of the SMOS satellite comprises, cf. Fig. 2
- the hexagonal satellite body,
- the solar panels, and
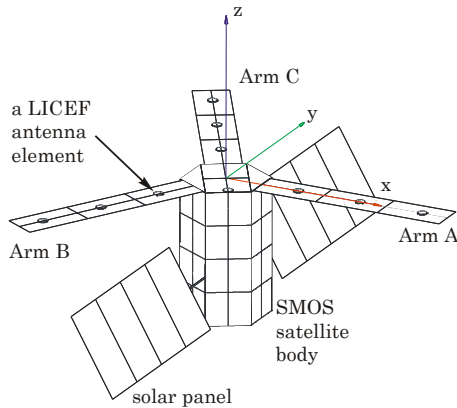- the Y-shaped LICEF antenna.

Figure 2. The applied SMOS model illustrating 10 of the 69 LICEF antenna elements. The solar panels are rotated 30° from their nominal (vertical) position.

The height of the satellite is 2293 mm (10.8λ) and the total end-to-end length of the solar panels is 9646 mm (45.5λ). The LICEF antenna elements are circular elements with a diameter of 145 mm embedded in the deployable arms and in the hub (the top face of the satel-

lite). Each arm has a length of 3340 mm (15.8λ), a width of 608 mm (2.9λ) and carries 23 elements. Of these 23 elements, 5 are on the hub and 18 on the arm, cf. Fig. 1. In total the LICEF antenna consists of 69 elements. The antenna elements are polarised in two orthogonal linear polarisations, H along the x-axis and V along the y-axis.

The scattering has been investigated for both polarisations of the selected set of antenna elements shown in Fig. 2. Results are presented here only for antenna element B_19, H-polarised, and only the co-polar field components are shown. B_19 is element No. 19 on arm B, the third-last antenna element on arm B in Fig. 1, the outmost of the elements in Fig. 2.

3.   SCATTERING ANALYSIS

3.1.   Source Modelling

The radiation of each antenna element will depend on the geometry in which the element is embedded. Thus, the elements in the hub must be modelled separately while the elements on the same arm may all be assumed to have the same radiation pattern. Different models shall, however, be applied for the antenna elements on the different LICEF arms as the arms are differently oriented with respect to the H and V polarisations.

A single LICEF antenna element in a segment of the supporting arm with further five passive elements have been modelled in details with MoM and compared to measurements and an excellent agreement has been found [2].

This MoM model has been simplified for the present project. A Gaussian beam has been chosen as a simple model for the free space antenna element. The beam width has been adjusted to that measured for the actual antenna element. This source model is next positioned 50 mm above the centre of a square box modelling a section of the LICEF antenna arm. The side length and the thickness of the box equal the width and the thickness of the antenna arm (respectively 608 mm and 80 mm). It has been demonstrated that the MoM model of this box with the simple antenna model yields a good representation especially of the backward radiated field when compared to the detailed MoM model. The backward radiated field is important as it is this field which illuminates the scattering structures.

An example on a full spherical pattern of an element on Arm B is shown in Fig. 4 (when the black regions are ignored). The directivity of the antenna element is 10.4 dBi.

The same Gaussian beam model is applied for the antenna elements on the hub. The scattering in the hub is

modelled by GTD as diffraction in the near edge of the hub. It is only by this diffracted field that the hub elements illuminate the solar panel. A MoM model is not applicable here as the model will be too large a source for application of GTD in the following scattering calculations.

3.2. Scattering Determined by MoM

The body of the satellite is too small in terms of wavelengths to the scattering may be determined by GTD and the body is therefore modelled in MoM.

An example on the field scattered from the satellite body is shown in Fig. 3 when the source is element B_19. The field contribution generating the shadow behind the satellite is seen in the direction $\phi = 60°$, the reflection is in the opposite direction at $\phi = -120°$ (standard spherical coordinates, cf. Fig. 2).
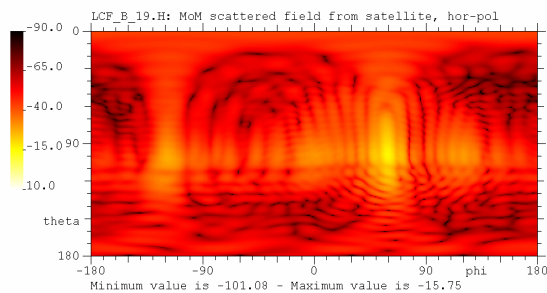

Figure 3. The co-polar component of the field scattered in the satellite body when illuminated by antenna B_19. Colour scale at left in dBi of the source antenna.

3.3. Scattering Determined by GTD

The scattering in the large solar panels are determined by GTD. The field is then generated ray by ray. First, rays are emitted from the source element in all directions determining the direct field. When shadows occur then shadowing – and therefore illuminated – objects are identified. Next, these objects are in turn included as GTD scatterers, and reflected and diffracted fields of 1st order are determined. Again, if shadows occur for these rays new scattering objects are identified and now reflected and diffracted fields of 2nd order may be determined. The procedure shall be repeated until the power of the scattered rays is negligible. In the present case 1st order diffractions and all multiple reflections are included.

The direct field of antenna element B_19 is shown in Fig. 4. The two shadowed regions are due to the solar panels which therefore shall be included as scatterers for 1st order reflections and diffractions.

The satellite body shall not be included here as the scattering in this was handled by MoM. But for higher order reflections and diffractions the satellite body must be included.
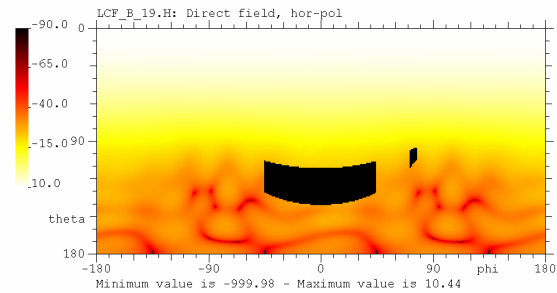

Figure 4. The co-polar component of the direct field from antenna B_19 with shadows of the solar panels.

In Fig. 5 the total field from element B_19 scattered in the solar panels is shown. The solar panels are in their nominal, vertical position (parallel to the yz-plane). The fields reflected in the solar panels appear within regions like the shadows in Fig. 4 but mirrored in $\phi = 90°$, i.e. for $\theta \cong 120°$ around $\phi = \pm180°$. The horizontal bands (also at $\theta \cong 120°$) represent diffractions in the vertical edges while diffractions in the horizontal edges of the nearest solar panel spread over most of the far-field sphere causing ripples as they interfere. Within the black 'wing' at $(\theta,\phi) \cong (50°,120°)$ these diffractions are shadowed by arm B which causes new reflections around $(\theta,\phi) \cong (130°,120°)$ but these are hardly distinguishable in the plot.
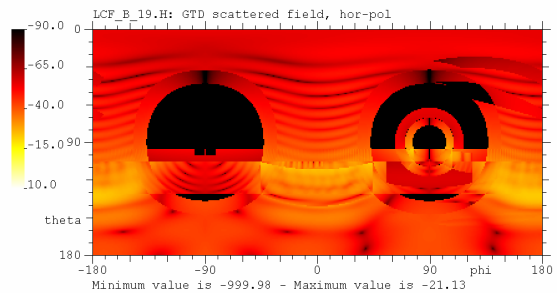

Figure 5. Field from antenna B_19 reflected and diffracted in the solar panels, co-polar field component.

A similar field pattern is shown in Fig. 6, but now with the solar panels rotated to 36° (in Fig. 2 the solar panels are shown at 30°). The diffractions in the rotated end edges of the panels now appear as curved bands across the sphere while the diffractions in the horizontal edges together with the reflections increase the field in a broad region around $\phi = 0°$, $\theta > 120°$.
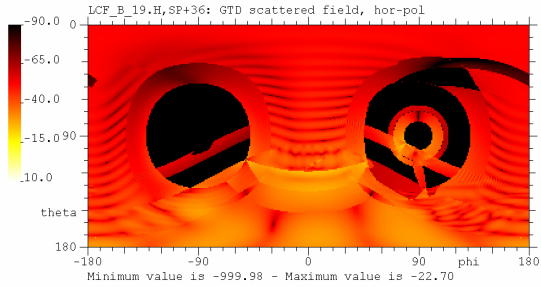
Figure 6. Field from antenna B_19 diffracted in the solar panes rotated to +36°, co-polar field component.

3.4. Total Fields

The total scattered field is obtained by adding all the MoM and GTD contributions apart from the direct GTD field from the antenna. For the H-polarised antenna B_19 this field is shown in Fig. 7 for the solar panels in nominal position (0°) and in Fig. 8 when the solar panels are rotated to 36°. The characteristics of both the MoM field (Fig. 3) and the GTD fields (Figs. 5 and 6) are found in these total scattered fields.
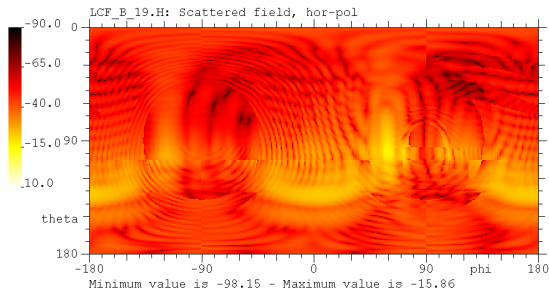

Figure 7. Total scattered field from antenna B_19, co-polar field component. Solar panels in nominal position.
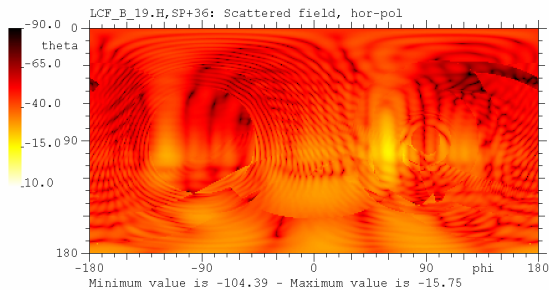

Figure 8. Total scattered field from antenna B_19, co-polar field component. Solar panels at 36°.

The total field is obtained by adding the total scattered field to the direct field, Fig. 4. This total field is shown in Fig. 9 for the solar panels in their nominal position. The effect of scattering in the satellite body is observed as ripples in the pattern in the region around $\phi=60°$ and

$\theta=110°$ while the overall fast ripples are caused by the scattering from the solar panels.

The total field for the solar panels rotated to 36° is shown in Fig. 10. The ripples and their intensity change according to the strength of the scattered fields but the pattern is not seriously influenced by the rotation of the solar panels.
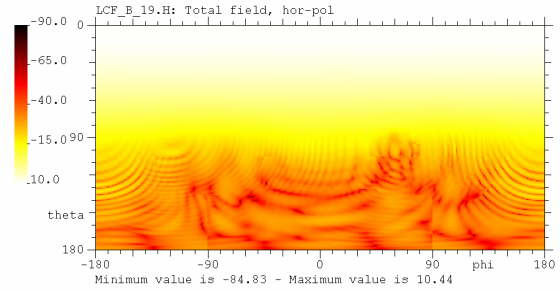

Figure 9. The total field of antenna B_19 with the scattering in the complete satellite, co-polar field component. Solar panels in nominal position.
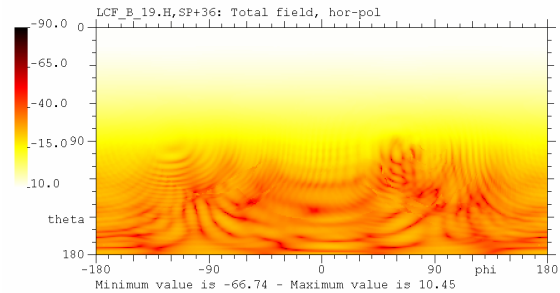

Figure 10. The total field of antenna B_19 with the scattering in the complete satellite, co-polar field component. Solar panels at 36°.

4. SUN SUPPRESSION PATTERNS

The antenna is sensitive to the noise received from the sun and therefore the antenna pattern in direction to the sun has been determined as function of time for different seasons.

Further, the solar panels may be at a fixed position (0°) or they may be rotated to follow the direction to the sun. This direction changes as the satellite circles the earth and it further depends on the season. The solar panels shall thus be re-oriented for each satellite position and the field value shall be determined in the actual direction to the sun.

The direction to the sun (the far-field direction for the antenna) and the orientation of the solar panels are given from orbital data. The direction to the sun varies

up to ±35° from the nominal direction (θ,φ) = (90°,0°). The directions to the sun for one orbit in December is shown in Fig. 11.
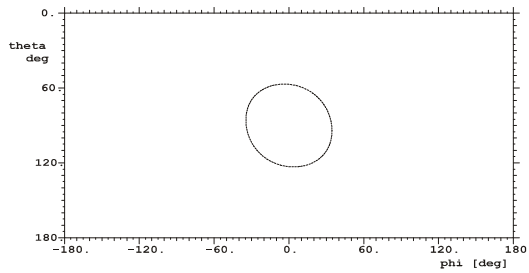

Figure 11. The direction to the sun during one orbit in December.

The co-polar field intensity, determined as a pattern value, is shown in Fig. 12 (black curve) as function of time, t, for the December orbit shown in Fig. 11, i.e. while the satellite is circling the earth the direction to the sun follows the curve in Fig. 11 and for the case with fixed solar panels the field values in direction of the sun can be read along this curve projected onto the pattern of Fig. 9.

The absence of field values between t = 1000s and 2000s are due to an occultation, the sun is behind the earth.

When the solar panels shall follow the direction to the sun for maximum sun illumination then the panels will rotate from -22° (at t = 0s) over 0° to 33° (at t = 2200s) and back over 0° to -33° (at t = 5200s) for finally to end at 22°.

The co-polar field intensity is then shown in Fig. 12 (red curve) for the considered orbit. It is seen that the orientation of the solar panels only has a little qualitative influence on the pattern for this orbit and this antenna element.
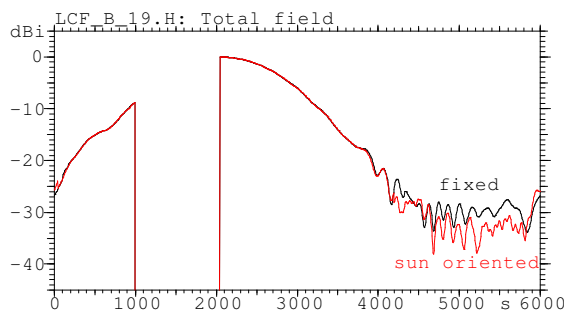

Figure 12. Co-polar field value in direction of the sun for orbiting satellite with fixed (black) and sun oriented (red) solar panels for an orbit at December solstice.

The same conclusion has been found for the other antenna elements of both polarisations and for the other orbits all over the year. For some of the cases the difference is below 1 dB, for other cases large differences are seen but always at levels 30 to 40 dB below peak of the free space antenna pattern.

5. CONCLUSIONS

A fast and reliable model for scattering in a complicated and dynamic satellite structure has been developed. The radiation from the source elements and their nearby surroundings has been determined by MoM and so has the scattering from the body of the satellite.

The MoM modelled source elements and their surroundings are sufficiently small to be considered as point sources when illuminating the solar panels and the scattering in these may be determined by GTD. This calculation method is fast which has importance as the scattering have been determined as function of time when the satellite is orbiting and the solar panels rotate to obtain optimum sun illumination. The overall computation time is short though a new ray tracing has to be carried out for each time step in the dynamically varying structure.

By these methods, the noise from the sun scattered in a complicated geometry of an orbiting satellite has been evaluated with emphasis on the consequences of rotating the solar panels versus having stationary panels. The conclusions of the performed orbit analyses are that the scattering in the solar panels in all cases is small, 25 dB below peak or lower and qualitatively independent on the orientation of the solar panels. The largest noise contribution from the sun is the direct illumination into the antenna elements.

6. ACKNOWLEDGEMENT

7. REFERENCES

1. Jensen F. and Pontoppidan K., *Assessment of the Impact of the SMOS Satellite Structure and Solar Panels on the LICEF Antenna Pattern and the Effects on Sun Suppression*, TICRA Final Report S-1361-02, September 2005.
2. Pivnenko S., Nielsen J.M., Kim O.S. and Breinbjerg O., *SMOS Antenna Measurements. Phase C/D Investigatory Measurements Report. No.: SO-TR-DTU-ANT-0004*. Report R725, Ørsted.DTU, Electromagnetic Systems, Technical University of Denmark, October 2005.